Liquid Crystals
Publication details, including instructions for authors and subscription information:
http://www.informaworld.com/smpp/title~content=t713926090

Guided modes and surface plasmon-polaritons observed with a nematic liquid crystal using attenuated total reflection

K. R. Welford[a]; J. R. Sambles[a]; M. G. Clark[b]
[a] Department of Physics, University of Exeter, Exeter, Devon, England [b] GEC Research, Wembley, Middlesex, England

To cite this Article Welford, K. R. , Sambles, J. R. and Clark, M. G.(1987) 'Guided modes and surface plasmon-polaritons observed with a nematic liquid crystal using attenuated total reflection', Liquid Crystals, 2: 1, 91 — 105

To link to this Article: DOI: 10.1080/02678298708086641

URL: http://dx.doi.org/10.1080/02678298708086641

LIQUID CRYSTALS, 1987, VOL. 2, NO. 1, 91–105

Guided modes and surface plasmon-polaritons observed with a nematic liquid crystal using attenuated total reflection

by K. R. WELFORD and J. R. SAMBLES
Department of Physics, University of Exeter, Exeter, Devon, England
and M. G. CLARK
GEC Research, East Lane, Wembley, Middlesex HA9 7PP, England

(*Received 7 July 1986; accepted 13 September 1986*)

An aligned layer of nematic liquid crystal with suitable optical anisotropy and under the application of appropriate applied voltages, may support various guided modes of light. Here the attenuated total reflection technique is used to examine such guided modes allowing simultaneous observation of the surface plasmon-polariton (S.P.P.) at a metal/liquid crystal interface. We report observations of the interaction between the bulk guided modes and the S.P.P., an interaction made possible by the strong refractive index anisotropy of the chosen liquid crystal. The influence of applied voltage upon the guided modes, the S.P.P. and their interaction is studied. Detailed reflectivity results are compared with theory for layered uniaxial media.

1. Introduction

The attenuated total reflection (A.T.R.) technique provides a very powerful method for examining guided modes in suitably fabricated dielectric layers. Consider a high index prism on which is deposited a thin low index layer, on top of which is the region of interest in which guiding may occur. Beyond the critical angle for total internal reflection in the prism there exists an evanescent field in the low index region which may couple the incident radiation in the prism to guiding modes in the layer of interest. At certain angles of incidence the momentum along the surface of the incident radiation will match the momentum of guiding modes in the layer and strong coupling will occur, see for example Tien [1]. This will result in a reduction of the reflected intensity from the incident beam. Hence by simply monitoring the reflectivity of a monochromatic light beam of low divergence as a function of the angle of incidence it is possible to characterize the guiding modes of the system and from the knowledge of coupling angles determine precise refractive index information.

Consider the particular geometry illustrated in figure 1. On the face of a high index prism is a thin layer of silver, on top of which is a thin layer of silicon oxide, which acts as an aligning layer for the region of interest, the nematic liquid crystal. On the top of this is placed a glass plate with an indium–tin oxide transparent electrode and a second aligning layer which induces the nematic director to align everywhere parallel to the bounding interfaces and the plane of incident radiation. This system is ideally suited to A.T.R. examination, the guided modes possible in the thin liquid crystal layer being excited by radiation tunnelling through the thin silver film for angles of incidence beyond the critical angle. Furthermore voltages may be applied between the silver film and the indium–tin oxide which changes the alignment of the

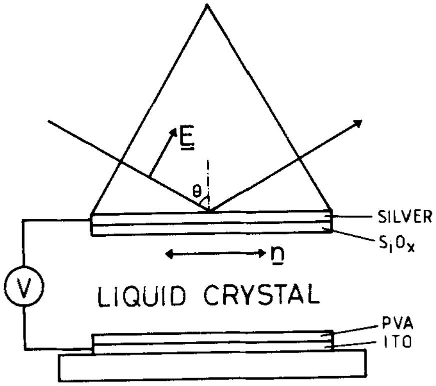

Figure 1. Experimental system. A schematic diagram of the layered structure investigated experimentally, showing the orientation plane of the nematic director and the incident radiation polarization.

liquid crystal director thus changing the guiding modes. Here we report the comparison between theoretical predictions and experimental data on the reflectivity for such a system providing an exacting test of models of nematic liquid crystals and the way they respond under the application of a low frequency voltage. Also, because the silver film supports a surface plasmon–polariton (S.P.P.) we report on novel results on simultaneous coupling of an S.P.P. and bulk modes in the liquid crystal layer. This may occur through the strong refractive index anisotropy of the liquid crystal coupled with the fact that under an applied voltage the liquid crystal layer near the surface changes far less readily than that in the bulk, leaving the S.P.P. undisturbed with the bulk modes significantly altered.

2. Experimental

A high index glass prism (n = 1·7942 at 632·8 nm) was coated with a thin ($\sim$ 40 nm) layer of high purity silver by conventional vacuum evaporation techniques. The rate of deposition of the silver layer was rapid ($\sim$ 1 nm s^{-1}) to ensure that a small grained optically smooth layer was achieved. The optical constants of this silver film may be determined accurately using the method of A.T.R., see Kretschmann [2]. Very briefly, this involves polarizing the incident radiation so that the **E**-field vector is in the plane of incidence (referred to as p polarized) and monitoring the internally reflected signal from the metal film as a function of angle of incidence. The evanescent waves generated in the metal film at angles greater than the critical angle of the system are able to couple to the S.P.P. mode at the metal–air interface. When the momentum of the wave along the metal interface matches that of the S.P.P. mode a resonant excitation occurs which results in an absorption of radiation from the incident beam. The reflected signal from the metal at angles close to the resonant condition shows a characteristic minimum. By adjusting the optical parameters of the metal layer in Fresnel's equations for a parallel sided metal film between two semi-infinite dielectrics it is possible to generate a theoretical curve which matches very closely the experimental data. In this way the complex dielectric constant ε and the thickness of the layer may be deduced. Following this procedure the optical constants of the silver layer in the investigation were found to be

$$\varepsilon = -17{\cdot}82 + 0{\cdot}77i, \quad d = 43{\cdot}6\,\text{nm}, \quad (\lambda = 632{\cdot}8\,\text{nm}),$$

which compares favourably with the results of other workers such as Gugger *et al.* [3]. In order to establish the accuracy of this analysis procedure the A.T.R. spectrum from the layer was also monitored at a second optical wavelength of 488·0 nm. Applying the same theoretical model in this case the optical parameters of the silver being found to be

$$\varepsilon = -8{\cdot}76 + 0{\cdot}48i, \quad d = 43{\cdot}9\,\mathrm{nm}, \quad (\lambda = 488{\cdot}0\,\mathrm{nm}).$$

The very close agreement between the metal layer thicknesses inferred by this method serves to establish its validity. The reflection spectra for the silver at both wavelengths are given in figures 2 and 3. The experimental apparatus for obtaining high quality computer controlled A.T.R. spectra is shown in figure 4 and is described elsewhere by Barnes and Sambles [4].

Having found the optical characteristics of the silver layer the silicon monoxide layer is evaporated on to the silver. The thickness of this layer is not a crucial parameter so long as it is thick enough to produce good uniform alignment of the nematic liquid crystal director and not so thick that the evanescent fields from the S.P.P. mode at the silver/silicon monoxide interface do not penetrate through the silicon monoxide with sufficient intensity. If that were the case any modification of the dielectric constant beyond the silicon monoxide layer would not be experienced by the S.P.P. mode. A typical evaporated thickness might be ~30 nm. What is a crucial factor, however, is the angle at which the evaporated beam of silicon monoxide arrives at the silver substrate. In order to produce good director alignment exhibiting strong surface anchoring characteristics and zero surface tilt Janning [5] showed that the material must be evaporated at an angle of 60° from the substrate normal. The use of conventional vacuum evaporating apparatus is quite sufficient to deposit the material. Although silicon monoxide is used as the evaporant it does undergo an amount of oxidation in the evaporation process which results in the exact stoichiometry being indeterminate. The material, as an aligning layer, is often referred to as SiO_x where $1 \leqslant x \leqslant 2$. Its aligning properties arise from its surface geometry which is corrugated in nature, see for example Geszti and Gosztola [6]. This does mean, however, that the surface is rather rough. To a first approximation the coating may be modelled as a parallel sided layer of isotropic material. The increase in dielectric constant close to the silver layer may be expected to affect the properties of the S.P.P. mode. If the A.T.R. spectra of this bilayer is monitored the resonance minimum in the reflection spectra is seen to have shifted to higher incident angles, which infers that the momentum of the S.P.P. mode has increased. Again, given that the optical parameters of the silver are known, the bilayer may be modelled by Fresnel's equations and the optical parameters of the SiO_x layer may be determined. The results of performing this fitting procedure on the A.T.R. spectrum of the bilayer system at both 632·8 nm and 488·0 nm are in good agreement with each other, yielding

$$\varepsilon = 3{\cdot}249 + 0{\cdot}002i, \quad d = 23{\cdot}8\,\mathrm{nm}, \quad (\lambda = 632{\cdot}8\,\mathrm{nm})$$

and

$$\varepsilon = 3{\cdot}108 + 0{\cdot}005i, \quad d = 23{\cdot}8\,\mathrm{nm}, \quad (\lambda = 488{\cdot}0\,\mathrm{nm}).$$

The A.T.R. spectra for the silver/SiO_x layered structure at 632·8 nm is presented in figure 5. A distinct systematic error is seen on close inspection of this figure, namely the theoretical prediction of the reflectivity around the resonance minimum is poor, particularly in the minimum where there appears to be more radiation being detected than expected. The reason for this is rather simple. The two major loss processes

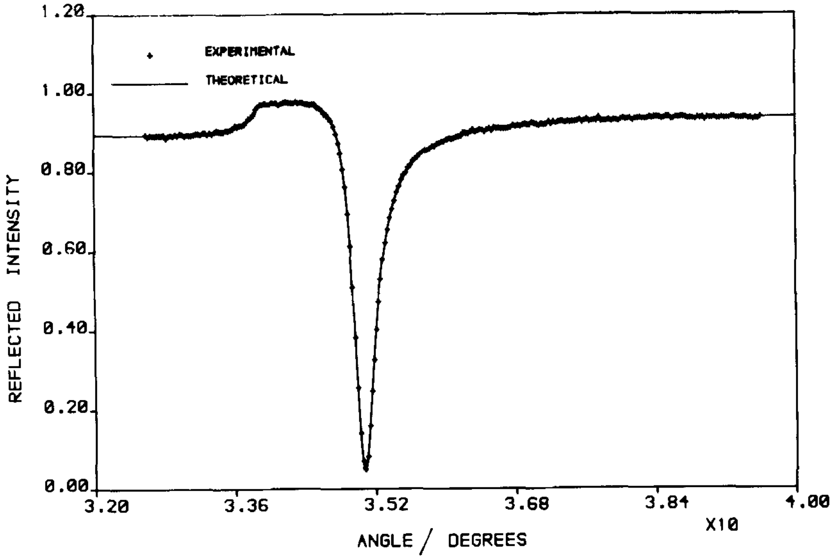

Figure 2. A.T.R. spectrum from the silver layer at the He–Ne wavelength (632·8 nm). The prism refractive index is 1·794 and the fitted parameters for the silver layer are $\varepsilon = -17{\cdot}82 + 0{\cdot}77i$ with thickness 43·6 nm.

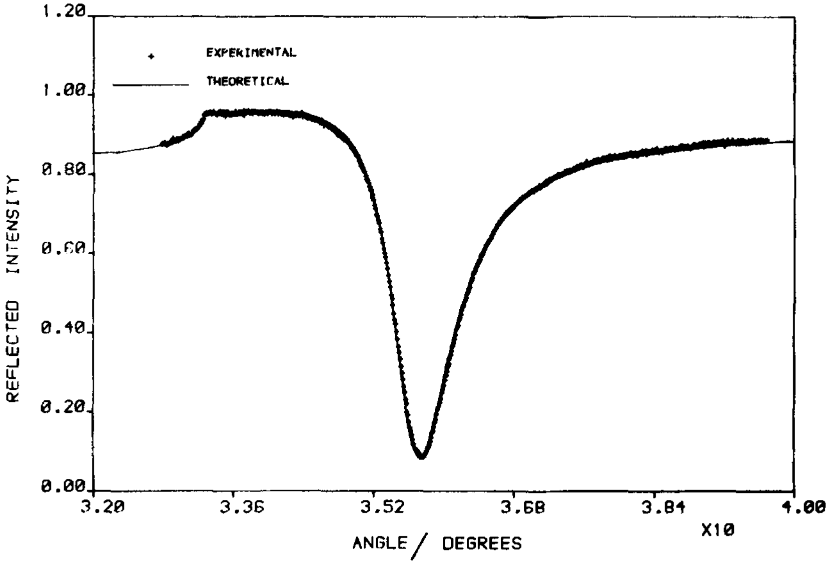

Figure 3. A.T.R. spectrum from the silver layer at a wavelength of 488 nm. The prism refractive index is 1·823 and the fitted parameters for the silver layer are $\varepsilon = -8{\cdot}76 + 0{\cdot}48i$ with thickness 43·9 nm.

contributing to the decay of the S.P.P. mode are Joule heating and evanescent coupling back into radiative bulk modes in the prism. Both of these mechanisms are built into the Fresnel equations and are therefore inherent in the theoretically predicted spectra. However, the SiO_x layer is far from smooth which allows a third loss mechanism, that of roughness coupled re-radiation. Basically, the S.P.P. mode is capable of decaying into bulk modes in the air and prism semi-infinite media by

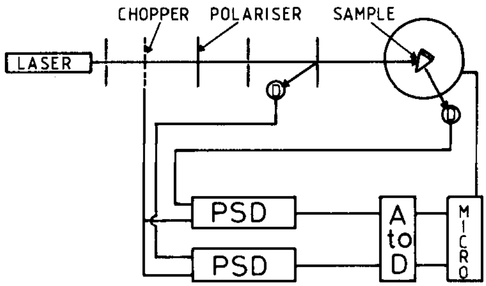

Figure 4. Experimental apparatus. Schematic diagram of the computer controlled A.T.R. system. The incident radiation is modulated, polarized and collimated, before interacting with the sample. The angle of incidence is controlled by the microcomputer and the reflected intensity is monitored by a photomultiplier detector, D. The reflected intensity and the reference intensity are phase sensitively detected and converted to digital information to be recorded by the microcomputer.

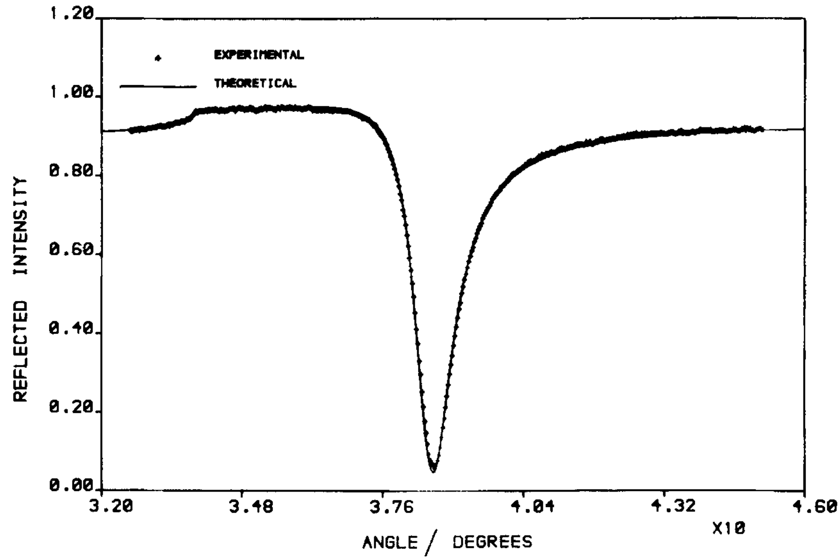

Figure 5. A.T.R. spectrum from the silver–SiO$_x$ bilayer system at a wavelength of 632·8 nm, demonstrating the systematic difference between theory and experiment due to roughness coupled re-radiation. The fitted parameters for the SiO$_x$ layer are $\varepsilon = 3{\cdot}25 + 0{\cdot}002i$ and thickness 23·8 nm.

momentum matching through the roughness profile. Hence the amount of radiation returned to the prism is enhanced by this mechanism, a mechanism not included in Fresnel's equations. The angle range over which the effect is expected to be most pronounced is where the S.P.P. **E**-fields are strongest, i.e. in the resonance minima of the A.T.R. spectra. It might be reasonable to assume that the re-radiated energy from the S.P.P. via this mechanism is approximately inversely proportional to the reflectivity response, i.e. strongest in the resonance minimum and weakest where the S.P.P. mode is least excited. The roughness coupled re-radiation from a S.P.P. mode has been extensively studied by many workers [7, 8]. If the reflectivity response of the bilayer is taken to be $R(\theta)$ then the re-radiated intensity is taken to be $A(\theta)$ where

$$A(\theta) = \alpha(1 - R(\theta))$$

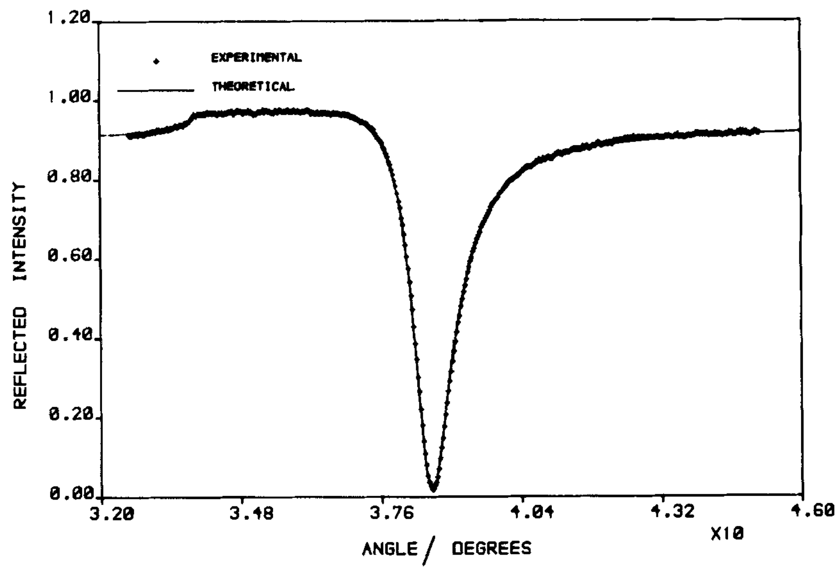

Figure 6. A.T.R. spectrum from the silver–SiO_x bilayer at a wavelength of $632{\cdot}8$ nm with roughness coupled re-radiation compensated for. The fitted parameters for the SiO_x are $\varepsilon = 2{\cdot}61 + 0{\cdot}02i$ with thickness $28{\cdot}8$ nm.

and α is a proportionality constant. By modifying the experimental data so that this extra radiation is removed the optical constants of the SiO_x layer may be redetermined.

The experimental reflection spectra are expected to be the theoretically predicted spectra, $R(\theta)$, but with the re-radiation term added into it. If the spectra obtained experimentally is denoted by $R'(\theta)$ then,

$$\begin{aligned} R'(\theta) &= R(\theta) + A(\theta), \\ &= R(\theta) + \alpha(1 - R(\theta)), \end{aligned}$$

which may be inverted giving the reflectivity spectra in the absence of the re-radiation loss mechanism as simply

$$R(\theta) = \frac{R'(\theta) - \alpha}{1 - \alpha}.$$

By removing the re-radiation loss mechanism in this way a value of α can be established which allows a better agreement of the theoretical spectra with the experimental data. The corrected A.T.R. spectra for both $\lambda = 632{\cdot}8$ nm and $\lambda = 488$ nm are presented in figures 6 and 7 with theoretical fits which yield for the SiO_x

$$\varepsilon = 2{\cdot}612 + 0{\cdot}020i, \quad d = 28{\cdot}8\,\text{nm}, \quad (\lambda = 632{\cdot}8\,\text{nm})$$

and

$$\varepsilon = 2{\cdot}685 + 0{\cdot}024i, \quad d = 28{\cdot}2\,\text{nm}, \quad (\lambda = 488\,\text{nm}).$$

These results do not agree with the SiO_x parameters determined by Rivere and Roger [9]. However, the layer thickness determined by the two independent spectra are in good agreement and the dielectric constant falls between the values for pure

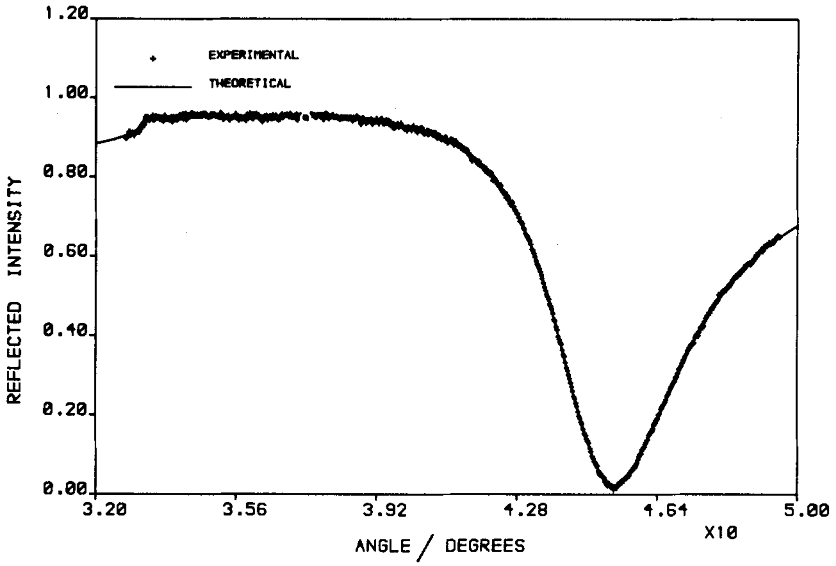

Figure 7. A.T.R. spectrum from the silver–SiO_x bilayer at a wavelength of 488 nm with roughness coupled re-radiation compensated for. The fitted parameters for the SiO_x layer are $\varepsilon = 2{\cdot}60 + 0{\cdot}02i$ with thickness 28·2 nm.

SiO (4·00) and pure SiO_2 (2·13). In Rivere and Roger's work an S.P.P. technique on a thin gold film covered with SiO_x determined the dielectric constant of the SiO_x layer to be approximately 1·67, which is very low. They attributed their findings to the fact that the SiO_x layer is very porous and hence because much of the layer was postulated to be air space the effective dielectric constant would be reduced. Our experimental results do not appear to demonstrate this effect.

Having fully characterized the surface layers on the glass prism, a nematic layer is confined between the prism and a glass plate held away from the prism by 6 μm mylar spacers. In order to produce a monodomain nematic layer the surface of the glass plate is coated with rubbed PVA. This serves to align the director parallel to the direction of the rubbing but with a small surface tilt which eradicates any problems due to reverse tilt disclinations. The glass plate used in this fabrication has a transparent conducting surface of indium–tin oxide. The nematic layer is guaranteed to be parallel sided (to better than $0{\cdot}5\,\mu m\,cm^{-1}$) by ensuring that the glass substrates used are optically flat and that the cell fabrication is carried out in a clean room environment (class 5000 or better). The A.T.R. spectra from this multilayer structure is now studied under the influence of various voltages applied between the silver layer and the indium–tin oxide layer. Since the liquid crystal material [10] is electrolytically damaged by applying a d.c. electric field an a.c. field is applied to the cell. Provided the frequency of the applied field is greater than the response time of the liquid crystal material the system will respond to the r.m.s. value of the applied field. The driving field frequency used in these experiments was fixed at 20 kHz. The typical optical response of this nematic layered structure under the influence of various applied voltages is shown in the A.T.R. spectra presented in figures 8 (*a*)–(*c*). Here the 0 V, 6·48 V and 20 V response functions are seen. The solid curve is the theoretically predicted spectrum and the crosses are the experimental data.

3. General discussion of results

Initially it had been anticipated that application of an a.c. voltage, greater than the critical voltage for the liquid crystal would largely serve to alter the effective refractive index of the liquid crystal by changing the director orientation with respect to the *p* polarized wave, thus changing the S.P.P. resonance.

Consider the Kretchmann–Raether geometry utilized. Next to the silver is firstly SiO_x which as is seen from figure 6 takes the S.P.P. resonance to a higher angle, the effective ε of the SiO_x/air region being higher than air alone. Then if we replace the air with liquid crystal whose index is of order 1·55 we may anticipate an even higher coupling angle for the S.P.P., as is seen in figure 9. Now on application of an a.c. field

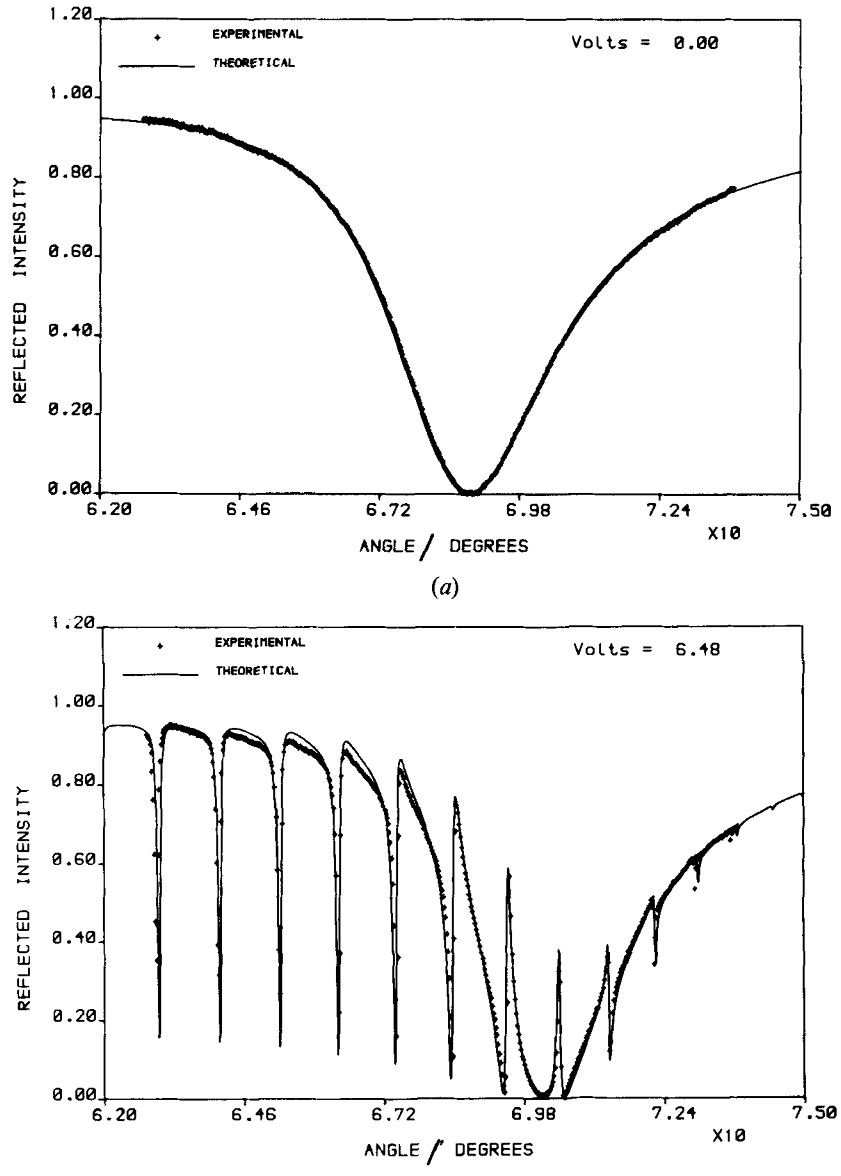

(*a*)

(*b*)

Figure 8.

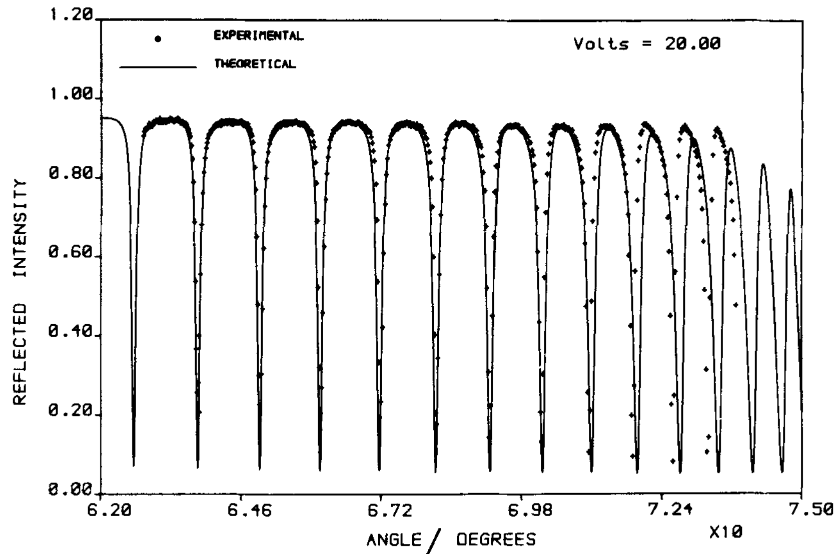

(*c*)

Figure 8. A.T.R. spectra from the liquid crystal cell represented in figure 1 at different applied voltages. Roughness coupled re-radiation has been compensated for. (*a*) 0 V, (*b*) 6·48 V, and (*c*) 20·0 V. In order to achieve a satisfactory fit to the experimental data illustrated in (*b*) the theoretical curve uses a somewhat higher voltage than measured experimentally (6·0 V). This may be associated with the ~ 3° tilt at the second surface for which no allowance has been made in the theory. The sharp resonance minima at roughly 1° spacing are associated with the guided waves in the nematic layer and the broader resonance minimum centred at ~ 70° in (*b*) is associated with the S.P.P. mode.

it was anticipated that the director of the liquid crystal would begin to tilt over from the homogeneous, zero voltage configuration, to the homeotropic, infinite voltage configuration. This should have the effect of moving the S.P.P. to still higher angles, since the effective refractive index rises towards 1·76. Sprokel *et al.* [11] have already observed this effect. Surprisingly, as is clear from figure 8 (*b*), this is not what happened. Instead at quite low voltages, just a little above threshold, a series of sharp minima appear, on the lower side of the S.P.P. resonance minimum. On further increase in voltage these move progressively across the S.P.P. resonance, the S.P.P. resonance itself remaining largely unaltered. This is illustrated clearly in figure 8 (*b*). On further increase of the voltage, which thickens the homeotropically aligned region the S.P.P. resonance starts to move off to the expected higher angle, the sharp minima remaining much more static, as illustrated in figure 8 (*c*). These guided mode effects were not observed by Sprokel *et al.* Given that the nematic layer they investigated was parallel sided it is difficult to see how the guided mode effects did not occur.

A simple quantitative explanation for these effects is clear. As the voltage is increased, the initial effect is to tilt the director over near the middle of the cell. For *p* polarized, or TM waves this means that a region of high refractive index (~ 1·76) lies between two regions of lower index (~ 1·55) giving a region which is able to support guided TM modes. (Note the TE index stays at 1·55 and thus no TE modes can be supported.) The electric field induced director deformation in the nematic material creates a type of graded index waveguide parallel to the interfaces. The sharp features seen in curves (*b*)–(*c*) of figure 8 are due to TM guided modes in the liquid crystal which are evanescently coupled to the incident radiation through the metal

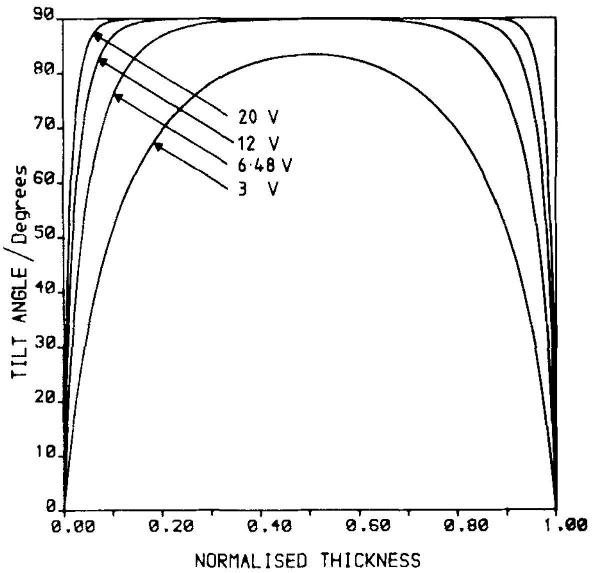

Figure 9. The tilt profiles of the nematic director under various applied voltages. The curves produced are for 3 V, 6·48 V, 12 V and 20 V. The profile becomes less sensitive to voltage variation the higher the voltage becomes.

film. The director tilt profile through the nematic layer is pictured in figure 9 for various applied voltages. At voltages close to the threshold voltage the director profile is significantly altered over much of the central region of the layer but little altered close to the boundary interfaces. Hence, because the electromagnetic fields associated with the S.P.P. mode decay exponentially over a length of typically a few hundred nanometers the S.P.P. mode is only slightly affected by the deformed nematic director profile. However, reorientation of the optic axis within the nematic material allows the exponentially decaying electromagnetic fields to couple to guided waves. Consequently, the S.P.P. resonance minimum is only shifted by ~ 1° when 6·48 V are applied but many guided modes are now supported by the structure. This is shown clearly in figure 8 (*b*). The sharp resonance minima at low angles of incidence (~ 63°) are not in a region where the S.P.P. mode is strongly excited. These guided modes are generated by the simple prism coupling technique which is already well understood (see Tien [1]). However at angles of incidence around the S.P.P. resonance minima (~ 70°) the coupling is via the electromagnetic fields of the S.P.P. mode. The guided modes in this region are seen (cf. figure 8 (*b*)) to have changed their character, the minima becoming inverted in the S.P.P. resonance minimum. A full understanding of why this should be is still not clear.

At higher applied fields the deformed director profile becomes more like a step index wave guide, again see figure 9. By this stage the change in the orientation of the optic axis close to the metal layer is significant and the S.P.P. mode is strongly modified. As seen in figure 8 (*c*) the S.P.P. mode is no longer excited within the investigated angle range and only the guided waves remain.

4. Detailed analysis of results

To be able to analyse fully these results two essential theories are needed. Firstly we need to be able to model the behaviour of the liquid crystal up to voltages several times threshold. Then having achieved this we need to model the optical properties by dividing the liquid crystal layer into a multilayered region and using Fresnel's equations for such a multilayered system to predict the reflectivity as a function of incidence angle.

Consider firstly the liquid crystal. Conventional models of the elastic response of an aligned liquid crystal to an applied electric field are usable up to a few times the threshold voltage (see Deuling [12]). While extrapolation methods are available for higher voltages (Clark *et al.* [13]) they are not satisfactory for predicting, with the required precision, the optical guiding properties of the current system. Thus to allow us to model this structure we have produced a theory of liquid crystal response, based on Deuling's work, which may readily be used to predict the director configuration for any voltage. This theory which assumes rigid surface bonding is presented in detail by Welford and Sambles [14]. Essentially the results we need for this work are

$$\frac{V}{V_0} = \frac{1}{\pi}(1 + Y(1 + \gamma))^{1/2} \times \int_0^\infty \left[\frac{(1 + Y)(1 + W) + \kappa YW}{((1 + Y)(1 + W) + \gamma YW)(1 + Y + W)(1 + W)W}\right]^{1/2} dW \qquad (1)$$

and

$$\frac{2z}{L}\int_0^\infty \left[\frac{((1 + Y)(1 + W) + \kappa YW)((1 + Y)(1 + W) + \gamma YW)}{(1 + Y + W)(1 + Y)(1 + W)W}\right]^{1/2} \frac{dW}{1 + W} = \int_0^{W_l} \left[\frac{((1 + Y)(1 + W) + \kappa YW)((1 + Y)(1 + W) + \gamma YW)}{(1 + Y + W)(1 + Y)(1 + W)W}\right]^{1/2} \frac{dW}{1 + W}. \qquad (2)$$

In these expressions V is the r.m.s. applied voltage, V_0 is the threshold voltage given by

$$V_0 = \pi\left[\frac{k_{11}}{\varepsilon_0(\varepsilon_\parallel - \varepsilon_\perp)}\right]^{1/2},$$

L is the cell thickness, z is distance through the cell, $Y = \tan^2\phi_m$ where ϕ_m is the maximum tilt angle and W_l is given by

$$W_l = \frac{\tan^2\phi(1 + Y)}{Y - \tan^2\phi}.$$

Further, $\kappa = (k_{33} - k_{11})/k_{11}$, $\gamma = (\varepsilon_\parallel - \varepsilon_\perp)/\varepsilon_\perp$, k_{11} being the splay deformation elastic constant, k_{33} the bend deformation elastic constant, $\varepsilon_\parallel\varepsilon_0$ the dielectric permittivity parallel to the director and $\varepsilon_\perp\varepsilon_0$ the dielectric permittivity perpendicular to the director. For given V we solve (1) to give Y and then substituting in (2) allows an accurate calculation of ϕ as a function of z. Thus for known elastic constants, permittivities, applied voltage and cell thickness we may predict the exact form of the director orientation in the cell. Having achieved this we now divide the cell into a large number of parallel slices by dividing ϕ_{max} by 45, giving 90 layers equally spaced in tilt but not in z thus preventing aliasing problems. Then to this 90 layer structure we add the known information about the SiO_x, the silver, the prism, the indium–tin oxide and the backing plate giving a complete dielectric layer model of the system. Then we need merely to utilize Fresnel's equations for a uniaxial medium for each layer to predict the overall reflectivity of the system. The theory needed for this is given by

Sprokel [15]. Essentially the reflection coefficient is given by

$$R = \frac{M_{21}}{M_{11}},$$

where

$$\mathbf{M} = \begin{bmatrix} M_{11} & M_{12} \\ M_{21} & M_{22} \end{bmatrix} = \prod_{j=0}^{j=N} [M_j]; \tag{3}$$

M_j being a matrix for each of the j regions, running from $j = 0$, the prism, to $j = N$, the last region but one, there being $N + 2$ regions of material (essentially the 0 region and the $N + 1$ region are semi-infinite).

Each M_j matrix takes the form

$$\begin{bmatrix} \dfrac{U_j + U_{j+1}}{2U_j} \exp(ik^+_{z,j}d_j) & \dfrac{U_j - U_{j+1}}{2U_j} \exp(ik^+_{z,j}d_j) \\ \dfrac{U_j - U_{j+1}}{2U_j} \exp(-ik^-_{z,j}d_j) & \dfrac{U_j + U_{j+1}}{2U_j} \exp(-ik^-_{z,j}d_j) \end{bmatrix},$$

d_j being the thickness of the jth layer, and U_j, $k^+_{z,j}$, $k^-_{z,j}$ are given by

$$U_j = \frac{\omega(\varepsilon_{x',j}\varepsilon_{z',j})^{1/2}}{(\omega^2 A_{22,j}\mu_0 - k_x^2)^{1/2}},$$

$$k^+_{z,j} = -\frac{A_{12,j}}{A_{22,j}} k_x + \frac{(\varepsilon_{x',j}\varepsilon_{z',j})^{1/2}}{A_{22,j}} (\omega^2 A_{22,j}\mu_0^2 - k_x^2)^{1/2}$$

and

$$k^-_{z,j} = \frac{A_{12,j}}{A_{22,j}} k_x + \frac{(\varepsilon_{x',j}\varepsilon_{z',j})^{1/2}}{A_{22,j}} (\omega^2 A_{22,j}\mu_0^2 - k_x^2)^{1/2}.$$

In these expressions, ω is the angular frequency of the radiation, k_x is the component of the incident wavevector in the x direction (i.e. along the layers of the system in the plane of incidence, $k_y = 0$). Also $\varepsilon_{x',j}$ and $\varepsilon_{z',j}$ are the components of the diagonalized uniaxial dielectric tensor for the jth layer, i.e.

$$\boldsymbol{\varepsilon}'_j = \begin{bmatrix} \varepsilon_{x',j} & 0 & 0 \\ 0 & \varepsilon_{x',j} & 0 \\ 0 & 0 & \varepsilon_{z',j} \end{bmatrix}$$

which is transformed, by use of the rotation matrix

$$\mathbf{R} = \begin{bmatrix} \cos\phi & \sin\phi \\ -\sin\phi & \cos\phi \end{bmatrix}$$

ϕ, being the tilt of the optic axis with respect to the x direction, to give, in the sample coordinate frame, the following expression relating **D** and **E**

$$\begin{bmatrix} D_x \\ D_y \end{bmatrix} = \begin{bmatrix} A_{11} & A_{12} \\ A_{21} & A_{22} \end{bmatrix} \begin{bmatrix} E_x \\ E_y \end{bmatrix},$$

with

$$\mathbf{A} = \mathbf{R}^{-1}\boldsymbol{\varepsilon}'\mathbf{R}$$

and so

$$\begin{aligned} A_{11} &= \varepsilon_{z'}\cos^2\phi + \varepsilon_{x'}\sin^2\phi, \\ A_{12} &= A_{21} = (\varepsilon_{z'} - \varepsilon_{x'})\sin\phi\cos\phi, \\ A_{22} &= \varepsilon_{z'}\sin^2\phi + \varepsilon_{x'}\cos^2\phi. \end{aligned}$$

Thus we may compute equation (3) from a knowledge of ε_j', ϕ_j, d_j for each layer and hence we are able to predict the angular dependent reflectivity for this system.

When the applied voltage is zero the nematic director profile is in an undeformed state and ϕ is everywhere close to 0°. (We ignore the $\sim 3°$ tilt induced at one surface by the PVA.) From a knowledge of the refractive indices of E7 (Harrison [16]), a theoretical fit to the experimental data can be obtained by allowing the optical parameter describing the SiO_x layer to be altered. The nature of the SiO_x layer means that it is rough and porous and an exact description of its optical parameters is not possible using Fresnel's equations. We saw previously that the effective optical properties of the SiO_x layer were determined using the S.P.P. resonance in air, Fresnel's equations, and a correction eliminating the effect of roughness coupled re-radiation. When the semi-infinite air is replaced by the liquid crystal it is reasonable to suppose that the interpenetration of the nematic material with the SiO_x layer will alter the effective optical parameters of the SiO_x layer. If the effective SiO_x layer thickness is maintained as 28·8 nm the effective dielectric constant is calculated to be

$$\varepsilon = 2{\cdot}50 + 0{\cdot}036i.$$

If we suppose that the spaces in the layer of SiO_x originally filled with air are now filled with the nematic material it would be reasonable to expect that the effective dielectric constant of the SiO_x would be increased. This has not occurred and must be interpreted as a consequence of applying an over-simplified model to the SiO_x layer. However, it should be noted that varying the thickness of the SiO_x by ± 10 per cent with consequential changes in the value for ε determined by fitting the zero voltage data has no significant affect upon the predicted reflectance curves at higher voltages. Here once again it has been necessary to remove the effect of the roughness coupled re-radiation. In this zero voltage case only the refractive indices of the material are important since the nematic director is in an undistorted state.

Nematic liquid crystal electrical, elastic and optical parameter values used in theoretical fitting of A.T.R. spectra.

Variable	Value
Ordinary index	2·3058, −0·0003
Extraordinary index	3·0240, −0·0004
Splay elastic constant	$11{\cdot}40 \times 10^{-12}\,\mathrm{Nm}^{-1}$
Bend elastic constant	$18{\cdot}20 \times 10^{-12}\,\mathrm{Nm}^{-1}$
Dielectric constant (parallel)	19·1000
Dielectric constant (perpendicular)	5·1200
Nematic layer thickness	8·97 μm

Using the electrical and elastic parameters for E7 given in the table theoretical A.T.R. spectra may be generated for other voltages which match the experimental spectra very closely. These fits we obtained by adjusting the thickness of the nematic layer and the supposed temperature of the nematic environment. The temperature of the nematic material determines the optical, electrical and elastic parameters of the material uniquely. The thickness of the nematic layer is found to be 8·95 ± 0·03 μm and the temperature of the layer was taken to be 17·8 ± 0·2°C. Tolerances on the nematic parameters for the demonstrated quality of theoretical fits varies from parameter to parameter. We find that the refractive indices have a rather critical effect upon achieving good theoretical agreement and allow a tolerance of ± 1 per cent at most. In contrast the fits are less sensitive to the other parameters and these may lie within a range of ± 3 per cent of those given. The theoretical A.T.R. spectra produced by Sprokel for comparison with his experimental data show no guided mode resonances. The reason for this is simply that Sprokel [15] modelled the nematic layer as semi-infinite on the basis that the S.P.P. electromagnetic fields penetrated only a fraction of the nematic thickness and could not interact with the furthest boundary layer. However, our work shows that the exponentially decaying fields are strongly influenced by the bulk reorientation of the nematic director.

5. Conclusions

We have examined the optical reflectivity of a layered system incorporating a silver film which may support an S.P.P. close to which is a nematic liquid crystal whose director may be influenced by the application of a voltage. The manner in which the reflectivity varies with angle for various applied voltages indicates not only the presence of the S.P.P. but also guided modes in the graded-index liquid crystal. Careful theoretical modelling of the liquid crystal director configuration as a function of applied voltage coupled with theory of the optical response of layered uniaxial media allows accurate predictions of the experimental reflectance curves. It is observed that the very sharp reflectivity minima found at quite low voltages are readily switched to a different angle by the application of a further small voltage yielding, at present, the ability to slowly modulate the reflected light intensity (~ 1 kHz at 80 per cent modulation). Currently more complex structures are being examined with a view to monitoring reflectance and transmittance in both parallel and twisted aligned cells.

K. R. W. thanks the SERC for a CASE award under which this research was commenced. J. R. S. thanks the SERC for a research grant with which some of the monitoring equipment for these experiments was purchased. The authors also wish to express thanks to Dr. Ken Harrison of R.S.R.E., Malvern, for his support, Mr. W. L. Barnes for help in producing theoretical reflectivity curves for multilayer systems, and Dr. T. W. Preist for aid in the mathematical modelling of the liquid crystal cell at high voltages.

References

[1] Tien, P. K., 1977, *Rev. mod. Phys.*, **49**, 361.
[2] Kretschmann, E., 1971, *Z. Phys.*, **241**, 313.
[3] Gugger, H., Jurich, M., Swalen, J. D., and Sievers, A., 1984, *Phys. Rev.* B, **30**, 4189.
[4] Barnes, W. L., and Sambles, J. R., 1986, *Surf. Sci.*, **177**, 399.
[5] Janning, J. L., 1972, *Appl. Phys. Lett.*, **21**, 173.
[6] Geszti, O., and Gosztola, L., 1986, *Thin Solid Films*, **136**, L35.
[7] Raether, H., 1982, *Surface Polaritons*, edited by V. M. Agranovich and D. L. Mills (North-Holland), chap. 9.
[8] Pockrand, I., 1978, *Surf. Sci.*, **72**, 577.
[9] Rivere, D., and Roger, G. R., 1983, *J. Phys., Paris*, **C10**, 113.
[10] BDH-E7: BDH Chemicals Ltd., Poole, Dorset, Nematic Eutectic Mixture, E7.

[11] SPROKEL, G. J., SANTO, R., and SWALEN, J. D., 1981, *Molec. Crystals liq. Crystals*, **68**, 29.

[12] DEULING, H. J., 1972, *Molec. Crystals liq. Crystals*, **19**, 123.

[13] CLARK, M. G., RAYNES, E. P., SMITH, R. A., and TOUGH, R. J. A., 1980, *J. Phys.* D, **13**, 2151.

[14] WELFORD, K. R., and SAMBLES, J. R., *Molec. Crystals liq. Crystals* (to be published).

[15] SPROKEL, G. J., 1981, *Molec. Crystals liq. Crystals*, **68**, 39.

[16] HARRISON, K., 1985 (private communication).